



CHORUS

This is the accepted manuscript made available via CHORUS. The article has been published as:

Thermal-to-electrical energy conversion by diodes under negative illumination

Parthiban Santhanam and Shanhui Fan

Phys. Rev. B **93**, 161410 — Published 25 April 2016

DOI: [10.1103/PhysRevB.93.161410](https://doi.org/10.1103/PhysRevB.93.161410)

Thermal-to-Electrical Energy Conversion by Diodes Under Negative Illumination

Parthiban Santhanam¹ and Shanhui Fan¹

Edward L. Ginzton Laboratory and Department of Electrical Engineering

Stanford University

Stanford, CA 94305

United States

We consider an infrared photo-diode under negative illumination, wherein the photo-diode is maintained at a temperature T and radiatively exposed to an emissive body colder than itself. We experimentally demonstrate that a diode under such conditions can generate electrical power. We show theoretically that the efficiency of energy conversion can approach the Carnot limit. This work is applicable to waste heat recovery as well as emerging efforts to utilize the cold dark universe as a thermodynamic resource for renewable energy.

The semiconductor photo-diode is widely used as a device for electrical power generation. In a typical configuration, a photo-diode at ambient temperature T is radiatively exposed to a hot surface with a temperature $T_{\text{surf}} > T$, which illuminates the diode with thermal radiation (Figure 1a, top). The diode absorbs the incident photons to generate electrical power. This configuration is used in both solar and thermo-photovoltaics.

In this Rapid Communication we investigate and experimentally demonstrate an alternative configuration through which a photo-diode can be used to generate electrical power. In this configuration, depicted in the bottom of Figure 1a, the diode is instead radiatively exposed to a cold surface with a temperature $T_{\text{surf}} < T$. We refer to a diode in such a condition as being under “negative illumination.”

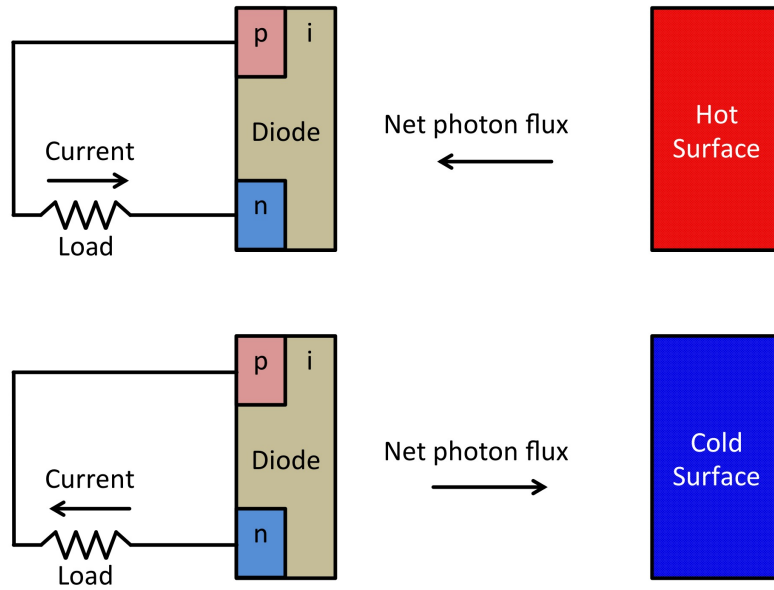
As we will show, an ideal photo-diode absorbing only within a narrow band can in fact, when placed under negative illumination from a cold surface $T_{\text{surf}} < T$, extract work from thermal energy at the Carnot limit $\eta_{\text{Carnot}} \equiv (T - T_{\text{surf}})/T$. We also report the results of a simple experiment on a real photo-diode and propose a model including non-idealities which agrees quite well with our measurements. We end this Rapid Communication by discussing the potential of this physical effect in the context of energy harvesting from the dark universe.

We begin our analysis of photo-diodes under negative illumination by applying the principle of detailed balance¹. For simplicity we first consider an ideal photo-diode with zero non-radiative recombination. We assume the diode is maintained at temperature T and is radiatively exposed to a perfectly absorptive surface at temperature T_{surf} over the entire hemisphere which it faces. We may express the current density J through such a diode in terms of the difference between the outgoing and incoming photon fluxes $J_{N,\text{out}}$ and $J_{N,\text{in}}$.

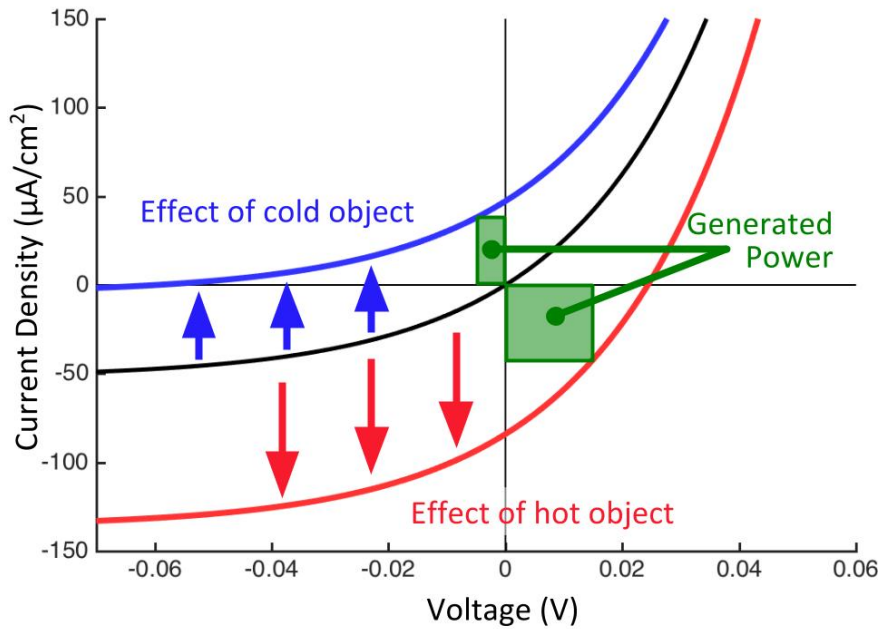
$$\begin{aligned}
 J &= q \cdot (J_{N,\text{out}} - J_{N,\text{in}}) \\
 &= \frac{q}{2\pi^2 c^2} \int_0^\infty d\omega \int_0^{\pi/2} d\theta \cos(\theta) \sin(\theta) \left[\frac{\omega^2}{e^{(\hbar\omega - qV)/(k_B T)} - 1} - \frac{\omega^2}{e^{(\hbar\omega)/(k_B T_{\text{surf}})} - 1} \right] \epsilon(\omega, \theta) \quad (1)
 \end{aligned}$$

where the emissivity ϵ is in general a function of angular frequency ω and polar angle θ , and we have invoked Kirchoff’s Law to set the diode’s absorptivity equal to its emissivity.

We apply Equation 1 to both the positive illumination regime, where $T_{\text{surf}} > T$, and the negative illumination regime, where $T_{\text{surf}} < T$; these regimes correspond to the illustrations at the top and bottom of Figure 1a respectively. Here we assume that $\epsilon(\omega, \theta) = \Theta(\omega - E_{\text{gap}}/\hbar)$



(a)



(b)

FIG. 1. (a) The upper diagram depicts the net inflow of photons from a hot surface giving rise to a reverse current in a conventional p - i - n photo-diode. The lower diagram indicates that the net outflow of photons to a cold surface can result in a positive current. (b) Current-voltage characteristics for a photo-diode exposed to an emissive surface with temperature below (blue), at (black), and above (red) that of the diode. The green shaded boxes represent the potential for electrical power generation in the two non-equilibrium scenarios.

with Θ being the unit step function and E_{gap} being the band gap of the semiconductor.

In [Figure 1b](#), the black curve passing through the origin represents the current-voltage relation when $T_{\text{surf}} = 295 \text{ K} = T$. [Equation 1](#) in this case gives rise to the well-known diode law. The red curve represents the relation when $T_{\text{surf}} = 315 \text{ K} > T$ (i.e. positive illumination). Here the greater flux of incident photons causes the generation rate of electrons and holes to exceed their recombination rate; thus a reverse current is seen when the diode's terminals are shorted. At open-circuit, an increased concentration of electrons and holes is required to raise the recombination rate to match the elevated generation rate. Thus a positive open-circuit voltage is obtained.

The blue curve in [Figure 1b](#) represents the characteristic current-voltage relation of the diode when $T_{\text{surf}} = 255 \text{ K} < T$ (i.e. negative illumination). With negative illumination, at short circuit the generation rates of electrons and holes fall short of their recombination rate, so that a forward current is seen. At open-circuit a reverse bias is now required to decrease the steady-state carrier concentrations to in turn decrease the recombination rate to match generation.

In both the cases of positive and negative illumination, at operating points between open-circuit and short-circuit the product JV is negative and corresponds to the generation of electrical power. The device is extracting work from the flow of heat across the temperature difference between one body at temperature T and another at T_{surf} . The existence of the operating regime explored here, in which the photo-diode acts as a heat engine located on the *hot side* of a temperature difference, has been alluded to multiple times in the existing literature but does not appear to have been analyzed in detail^{2,3}. In particular, the efficiency with which a diode could extract electrical work from thermal energy has not been analyzed and no experiments have been reported to verify the basic existence of the phenomenon. These items are therefore the primary aims of this Rapid Communication.

We may use [Equation 1](#) to calculate the energy conversion efficiency of an ideal diode under negative illumination. For each electronic charge that flows through the combined diode-load circuit, the amount of work extracted is $-qV$ and the amount of heat rejected is $\hbar\omega$, where q is the magnitude of the electron's charge and $\hbar\omega$ is the energy of an average photon emitted by the diode. Since the input energy is simply the sum of these two

quantities, we may express the thermal-to-electrical energy conversion efficiency as

$$\eta = \frac{-qV}{-qV + \hbar\omega}. \quad (2)$$

We compute the efficiency η when the emissivity of the diode is in the narrow band limit (i.e. $\epsilon(\omega, \theta)$ is only nonzero within a small window of frequencies around some ω_0)³. In this limit, setting $J = 0$ in Equation 1 yields the open circuit voltage

$$V_{\text{oc}} = \frac{\hbar\omega_0}{q} \left(1 - \frac{T}{T_{\text{surf}}} \right). \quad (3)$$

Near this open-circuit operating point then, η approaches the Carnot efficiency.

$$\eta_{\text{max}} = \frac{-qV_{\text{oc}}}{-qV_{\text{oc}} + \hbar\omega_0} = \frac{T - T_{\text{surf}}}{T} = \eta_{\text{Carnot}} \quad (4)$$

In principle the emissivity of a body can be tailored with a variety of photonic structures⁴⁻⁹ which could be utilized to approximate this narrow band limit. However because the maximum power point can be far from the open-circuit condition, a wide emissivity spectrum may prove more ideal in practice if the objective is to maximize the power generated.

We now present an experimental demonstration of the physics of a photo-diode operating under negative illumination. In particular we seek to demonstrate that when a photo-diode's field-of-view is covered by a highly emissive surface, the sign of the temperature difference ($T_{\text{surf}} - T$) determines the sign of the short-circuit current density $J(V = 0)$ as portrayed in Figure 1. Consequently when $(T_{\text{surf}} - T) < 0$ (i.e. when the photo-diode is placed under negative illumination) in the presence of a finite resistive load connected to the diode's terminals, the diode will operate in the second quadrant and therefore generate electrical power to drive the load.

The experimental setup is depicted in Figure 2. An uncooled HgCdZnTe photo-diode (Vigo's PVI-3TE-6), whose room-temperature bandgap E_{gap} is 218 meV, is set facing a temperature-controlled infrared-emissive surface (Acktar's Metal Velvet)¹⁰⁻¹². A hyper-hemispherical GaAs solid immersion lens is attached to the photo-diode's detecting surface so that the field of view is constrained to a cone with an 18° half-angle. The area of the diode's optical cross-section is a 1×1 mm² square. The emissive surface is placed close enough to the photo-diode that it covers the diode's entire field-of-view. The temperature

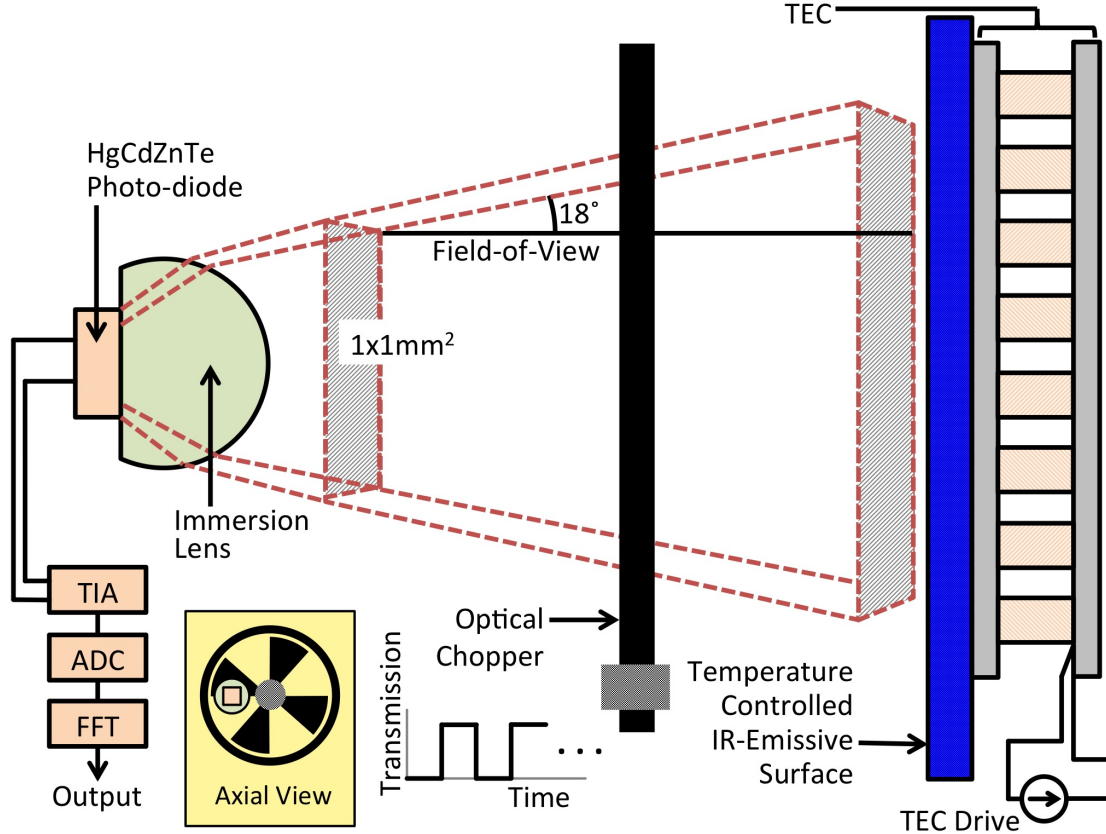


FIG. 2. Diagram of the experimental setup. An infrared photo-diode was exposed to a high-emissivity surface which covered its entire field-of-view. A chopper was used to allow a lock-in measurement of the photo-current.

of the emissive surface is varied from 285 K to 305 K while the temperature of the diode remains at 295 K, and the diode's short-circuit photo-current is measured.

In order to characterize the photo-current as a function of emissive surface temperature, a lock-in technique is employed. An optical chopper (415 Hz) is introduced between the diode and surface so that only during the open phase of the chopper is the diode optically exposed to the emissive surface. The diode is connected directly to a Trans-Impedance Amplifier (TIA) whose input impedance is negligible due to a virtual null. The photo-current is amplified with a total trans-impedance gain of 10^6 V/A; it also passes through broad band low-pass and high-pass filters to keep the amplifier from overloading. This amplified signal, two examples of which are shown in the main plot of [Figure 3](#), is then read in by an Analog-to-Digital Converter (ADC) at 10^5 samples/second for a duration of 1 second; this digital signal is subsequently post-processed using a Fast Fourier Transform (FFT). Note that both of the raw data signals in [Figure 3](#) resemble zero-mean square waves

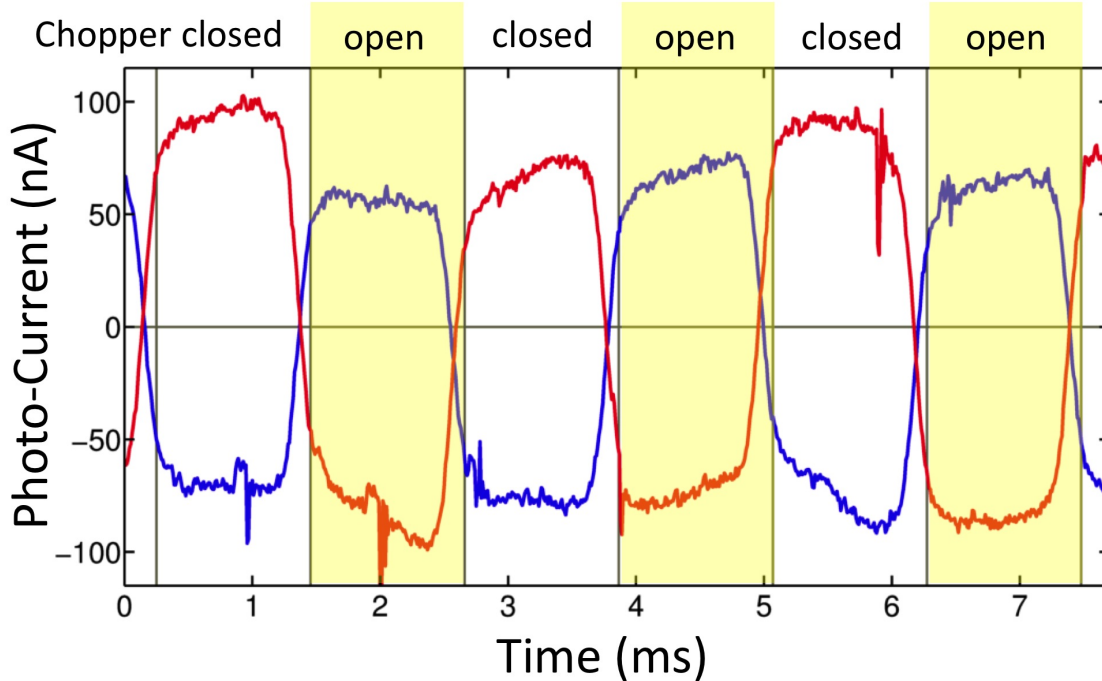


FIG. 3. Raw data from two photo-current measurements. Red and blue represent high and low emissive surface temperatures respectively.

because their DC components are filtered out to avoid saturating the TIA.

Before we examine the quantitative data produced from the FFT, it is useful to examine the raw data in [Figure 3](#) qualitatively. When the emissive surface is hot, as in the case of the red curve, the photo-current seen during the open phase of the measurement is approximately 150 nA below its value during the closed phase. During the open phase, the photo-diode experiences a net influx of photons from the hot surface; during the closed phase, it sees only the chopper blade with which it is in equilibrium. Thus we can infer that the effect of the hot surface is to produce a reverse current of 150 nA. By contrast when the emissive surface is cold, as in the case of the blue curve, the photo-current seen during the open phase of the measurement is about 130 nA above its value during the closed phase. Since the diode sees the cold surface during the open phase but only the chopper blade during the closed phase, we may infer that the effect of the cold surface is to produce a forward current of 130 nA. The distinctive 180° phase shift seen in [Figure 3](#) as T_{surf} changes from above T to below T

is the key feature of the measurement.

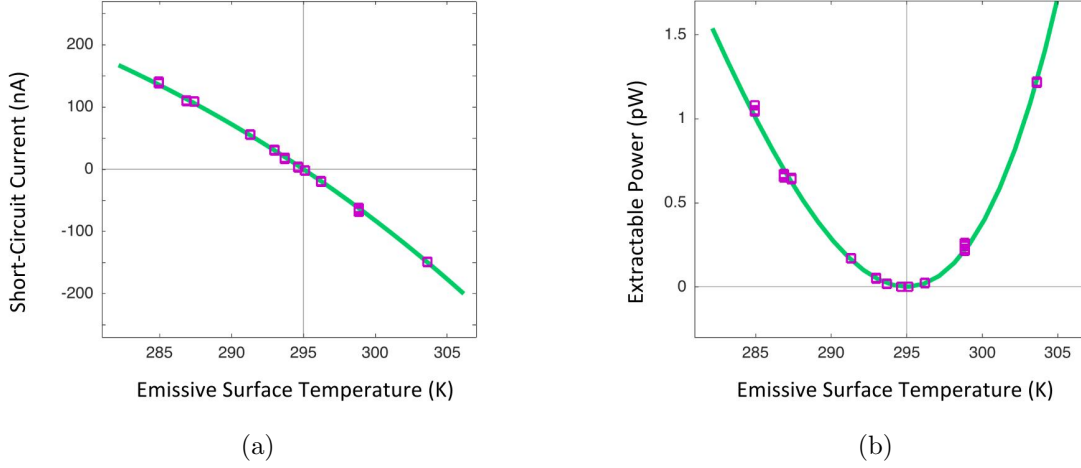


FIG. 4. (a) Short-circuit current and (b) extractable power versus temperature of the emissive surface facing the diode. The discrete points are the results of a lock-in measurement experiment described in the text. The solid line represents a model including non-idealities.

The short-circuit current I_{sc} was computed as the averaged peak-to-peak amplitude of the photo-current square wave in Figure 3 using an FFT algorithm. The zero-bias resistance of the diode was measured at equilibrium to be $R_{ZB} = 220 \Omega$, and the maximum extractable power is $P = \frac{1}{4} I_{sc}^2 R_{ZB}$. I_{sc} and P are plotted versus emissive surface temperature in Figure 4. When the emissive surface was colder than the diode, a positive photo-current was seen, but when the emissive surface was hotter than the diode, a negative photo-current was observed. In both cases the extractable electrical power is a positive quantity, indicating that the diode can generate electricity from a temperature difference of either sign.

Also included in Figure 4 are results from a theoretical model of a non-ideal diode, as represented by the following equation.

$$I = \frac{q \cdot A_{\text{optical}}}{4\pi^2 c^2} \cdot \left[\int_{E_{\text{gap}}/\hbar}^{\infty} \frac{\omega^2 d\omega}{e^{(\hbar\omega - q(V - IR_{\text{series}}))/(k_B T)} - 1} - \int_{E_{\text{gap}}/\hbar}^{\infty} \frac{\omega^2 d\omega}{e^{(\hbar\omega)/(k_B T_{\text{surf}})} - 1} \right] + \frac{V - IR_{\text{series}}}{R_{\text{shunt}}} \quad (5)$$

where A_{optical} is the effective optical area of the diode. R_{shunt} and R_{series} offer a convenient way to capture the effects of non-radiative recombination, finite carrier mobility, and finite contact resistance. R_{shunt} is equal to the product of the zero-bias resistance of an ideal diode of the same bandgap and the ratio of the radiative recombination lifetime to the non-

radiative lifetime. R_{series} is equal to the difference between the zero-bias resistance of the full device and the parallel combination of R_{shunt} with the zero-bias resistance of an ideal diode. A more complete model of electron transport in a photo-diode can be reduced to these two quantities insofar as the total extractable power is concerned. This is possible largely because unlike diodes under positive illumination, the maximum power point under negative illumination is at sufficiently low voltage that the current-voltage characteristic can be linearized.

Although it is possible to directly model a complete device and thereby generate values for R_{shunt} and R_{series} for use in Equation 5, doing so falls outside the scope of this work. Instead, R_{shunt} and R_{series} for the experiment presented previously were determined by the responsivity implied by the short-circuit current measurements in Figure 4a and an independent measurement of the zero-bias resistance of the diode. For the diode used in the experiment then $A_{\text{optical}} = 0.1 \text{ mm}^2$, $R_{\text{shunt}} = 23.4 \text{ } \Omega$, and $R_{\text{series}} = 197 \text{ } \Omega$. Note that the use of a solid immersion lens results in an A_{optical} exceeding the diode’s true physical area. As seen in Figure 4, the model agrees well with our measurements, including the asymmetry of extractable power between positive and negative temperature differences.

The model in Equation 5 can be used to evaluate and compare new designs in terms of their values for R_{shunt} and R_{series} . For an ideal device, $R_{\text{series}} = 0$ and $R_{\text{shunt}} = \infty$.

In the case of the non-ideal diode in our experiment, operating at 295 K while being optically exposed to a 285 K emissive surface led to just over 1 pW of extractable electrical power. In principle one could redesign the structure so its electrical contacts are much less than a diffusion length from all relevant radiative recombination. Such a change would lead to a nearly ideal short-circuit current and could be captured by our model via a significantly reduced R_{series} . If R_{series} could be effectively eliminated while R_{shunt} remained unchanged, our model predicts that a square decimeter of a 295 K surface exposed to the coldness of space at 3 K could generate more than a micro-watt of electrical power.

The shunt parasitic R_{shunt} in our model primarily reflects the presence of Auger recombination and its time-reversed process electron impact ionization (sometimes called Auger generation). The presence of these non-radiative processes is a fundamental aspect of any diode in any semiconductor with a narrow direct bandgap. In p -type $\text{Hg}_{1-x}\text{Cd}_x\text{Te}$, the Auger lifetime at low excitation is shorter than the radiative lifetime by a factor of $O(100)$ and accounts for the low R_{shunt} measured in our experiment¹³.

Moderate improvements of the model parameter R_{shunt} may be possible using techniques which have not been fully exploited here. One well-established method to reduce the relative strength of Auger processes is to employ quantum wells¹⁴. Potential also exists to exploit the Purcell effect using optical concentration in space and frequency; by enhancing the strength of radiative interactions in this way the relative importance of non-radiative processes can be diminished¹⁵. The use of a solid immersion lens in our experiment represents a step in this direction¹⁶. Furthermore, certain material systems under development are promising candidates for more efficient devices. For example, III-V semiconductor alloys with dilute concentrations of Nitrogen are known to have less Auger generation and recombination due to the increased effective mass of conduction-band electrons¹⁷.

One potential implication of the effect observed here lies in the extraction of power from the cold dark universe.^{2,18-30} Byrnes, et. al.² considered a power extraction scheme in which a heat engine extracts work from between the $T = 300$ K ambient and a radiatively cooled blackbody facing a 3 K cold reservoir. In the ideal limit, in which the heat engine is a Carnot engine, this system has a maximum power density of 48.4 W/m^2 . We emphasize that this result does not represent the fundamental limit of power extraction. This may be understood by noting the constraint in Ref. [2] that the radiatively cooled surface is a classical blackbody. Instead, if the body radiating into the 3 K cold reservoir is composed of several grey bodies with narrow emissivity spectra and the temperature of each body is then optimized independently, the maximum power density is 55.0 W/m^2 , which defines a multi-spectral limit³¹. If the negative illumination effect observed in this paper were exploited to extract power from the same two thermal reservoirs, [Equation 1](#) predicts a maximum power density of 54.8 W/m^2 in the ideal limit. This figure significantly exceeds that of the equilibrium isothermal configuration from Byrnes, et. al. and in fact is fairly close to the ideal multi-spectral limit.

In conclusion, we have analyzed a method for extracting electrical work from a hot body radiating into a cold optical far field, such as the Earth radiating into outer space, using a long-wavelength semiconductor photo-diode. In the ideal case we find that the thermal-to-electrical energy conversion efficiency approaches the Carnot limit and the maximum extractable power density from a 300 K object is found to be $\approx 55 \text{ W/m}^2$. An experimental test of the basic principle yielded good agreement with theory. The conceptual principle provides an opportunity to tap into a major unused source of renewable energy. Improved

devices with large emitting areas could have implications for off-grid power generation at night and waste-heat recovery.

This work was supported by the DOE “Light-Material Interactions in Energy Conversion” Energy Frontier Research Center under Grant No. DE-SC0001293.

REFERENCES

- ¹W. Shockley and H. J. Queisser, “Detailed balance limit of efficiency of p - n junction solar cells,” *Journal of Applied Physics* **32**, 510–519 (1961).
- ²S. J. Byrnes, R. Blanchard, and F. Capasso, “Harvesting renewable energy from Earth’s mid-infrared emissions,” *Proc. Nat. Acad. Sci. of the U. S. A.* **111**, 39273932 (2014).
- ³P. Berdahl, “Radiant refrigeration by semiconductor diodes.” *Journal of Applied Physics* **58**, 1369–1374 (1985).
- ⁴J.-J. Greffet, R. Carminati, K. Joulain, J.-P. Mulet, S. Mainguy, and Y. Chen, “Coherent emission of light by thermal sources,” *Nature* **416**, 61–64 (2002).
- ⁵J. G. Fleming, S. Y. Lin, I. El-Kady, R. Biswas, and K. M. Ho, “All-metallic three-dimensional photonic crystals with a large infrared bandgap,” *Nature* **417**, 52–55 (2002).
- ⁶M. U. Pralle, N. Moelders, M. P. McNeal, I. Puscasu, A. C. Greenwald, J. T. Daly, E. A. Johnson, T. George, D. S. Choi, I. El-Kady, and R. Biswas, “Photonic crystal enhanced narrow-band infrared emitters,” *Applied Physics Letters* **81**, 4685–4687 (2002).
- ⁷C. Luo, A. Narayanaswamy, G. Chen, and J. D. Joannopoulos, “Thermal radiation from photonic crystals: A direct calculation,” *Phys. Rev. Lett.* **93**, 213905 (2004).
- ⁸D. L. Chan, M. Soljacic, and J. D. Joannopoulos, “Direct calculation of thermal emission for three-dimensionally periodic photonic crystal slabs,” *Physical Review E* **74**, 1–9 (2006).
- ⁹X. Liu, T. Tyler, T. Starr, A. F. Starr, N. M. Jokerst, and W. J. Padilla, “Taming the blackbody with infrared metamaterials as selective thermal emitters,” *Phys. Rev. Lett.* **107**, 045901 (2011).
- ¹⁰S. A. VIGO System, “PVI-3TE series data sheet: 2-12 μm IR photovoltaic detectors, thermoelectrically cooled, optically immersed,” (2015).
- ¹¹G. L. Hansen, J. L. Schmit, and T. N. Casselman, “Energy gap versus alloy composition and temperature in $\text{Hg}_{1-x}\text{Cd}_x\text{Te}$,” *Journal of Applied Physics* **53**, 7099–7101 (1982).
- ¹²Acktar, “Metal Velvet coated foil data sheet.” Product catalog. (2014).
- ¹³T. N. Casselman, “Calculation of the auger lifetime in p -type $\text{Hg}_{1-x}\text{Cd}_x\text{Te}$,” *Journal of Applied Physics* **52**, 848–854 (1981).
- ¹⁴L. C. Chiu and A. Yariv, “Auger recombination in quantum-well InGaAsP heterostructure lasers,” *IEEE Journal of Quantum Electronics* **QE-18**, 1406–1409 (1982).
- ¹⁵Z. Yu, G. Veronis, S. Fan, and M. L. Brongersma, “Design of midinfrared photodetectors

- enhanced by surface plasmons on grating structures,” *Applied Physics Letters* **89**, 151116 (2006), 10.1063/1.2360896.
- ¹⁶Z. Yu, N. P. Sergeant, T. Skauli, G. Zhang, H. Wang, and S. Fan, “Enhancing far-field thermal emission with thermal extraction,” *Nature Communications* **4** (2013), 10.1038/ncomms2765.
- ¹⁷J. S. Harris, R. Kudrawiec, H. B. Yuen, S. R. Bank, H. P. Bae, M. A. Wistey, D. Jackrel, E. R. Pickett, T. Sarmiento, L. L. Goddard, V. Lordi, and T. Gugov, “Development of GaInNASb alloys: Growth, band structure, optical properties and applications,” *Physica Status Solidi B* **244**, 2707–2729 (2007).
- ¹⁸A. P. Raman, M. A. Anoma, L. Zhu, E. Rephaeli, and S. Fan, “Passive radiative cooling below ambient air temperature under direct sunlight,” *Nature* **515**, 540–544 (2014).
- ¹⁹F. Trombe, “Perspectives sur l’utilisation des rayonnements solaires et terrestres dans certaines régions du monde,” *Revue Générale Thermique* **6**, 1285–1314 (1967).
- ²⁰S. Catalanotti, V. Cuomo, G. Piro, D. Ruggi, V. Silvestrini, and G. Troise, “The radiative cooling of selective surfaces,” *Solar Energy* **17**, 83–89 (1975).
- ²¹C. G. Granqvist and A. Hjortsberg, “Radiative cooling to low temperatures: General considerations and application to selectively emitting SiO films,” *Journal of Applied Physics* **52**, 4205–4220 (1981).
- ²²P. Berdahl, M. Martin, and F. Sakkal, “Thermal performance of radiative cooling panels,” *International Journal of Heat and Mass Transfer* **26**, 871–880 (1983).
- ²³M. Martin and P. Berdahl, “Summary of results from the spectral and angular sky radiation measurement program,” *Solar Energy* **33**, 241 – 252 (1984).
- ²⁴B. Orel, M. Gunde, and A. Krainer, “Radiative cooling efficiency of white pigmented paints,” *Solar Energy* **50**, 477 – 482 (1993).
- ²⁵T. Nilsson, W. Vargas, G. Niklasson, and C. Granqvist, “Condensation of water by radiative cooling,” *Renewable Energy* **5**, 310–317 (1994).
- ²⁶A. H. H. Ali, I. Taha, and I. Ismail, “Cooling of water flowing through a night sky radiator,” *Solar Energy* **55**, 235 – 253 (1995).
- ²⁷T. M. Nilsson and G. A. Niklasson, “Radiative cooling during the day: simulations and experiments on pigmented polyethylene cover foils,” *Solar Energy Materials and Solar Cells* **37**, 93–118 (1995).
- ²⁸A. R. Gentle and G. B. Smith, “Radiative heat pumping from the earth using surface

- phonon resonant nanoparticles,” [Nano Letters](#) **10**, 373–379 (2010).
- ²⁹A. Gentle, J. Aguilar, and G. Smith, “Optimized cool roofs: Integrating albedo and thermal emittance with R-value,” [Solar Energy Materials and Solar Cells](#) **95**, 3207–3215 (2011).
- ³⁰E. Rephaeli, A. Raman, and S. Fan, “Ultrabroadband photonic structures to achieve high-performance daytime radiative cooling,” [Nano Letters](#) **13**, 1457–1461 (2013).
- ³¹P. Santhanam and S. Fan, (unpublished).